

Non-constant Diffusion Coefficients: Short Description of Modeling and Comparison to Experimental Results

John S. Petersen, Chris A. Mack, John Sturtevant, Jeffrey D. Byers and
Daniel A. Miller

JSP (Shipley Company), JS, JDB, DAM, SEMATECH, 2706 Montopolis Drive, Austin, TX,
78741-6499; CAM, FINLE Technologies, Inc., P. O. Box 162712, Austin, TX 78716

1. ABSTRACT

Chemical changes within a resist material (for example, resulting from the exposure and subsequent chemical reactions during post exposure bake) will in general, result in a change in diffusivity of components within that material. In the case of positive chemically amplified resists, the diffusivity of the photo-generated acid changes as a function of the extent of polymer deprotection. The deprotection reaction leads to the generation of small reaction product molecules, some of which are volatile. The liberation of these reaction products causes an increase in the free volume and changes in the chemical behavior in the exposed area. These changes, primarily the increase in free volume, results in an increase in the diffusivity of the acid. Low exposure areas have lower acid diffusivity, leading to a lower efficiency of reaction. This results in a contrast enhancement of the latent image due to the concentration dependent diffusivity of the acid.

In this paper, a concentration dependent diffusivity expression is incorporated into a lithography simulator to explore these effects on lithographic performance. Using the assumption of free volume, suitable expressions for the diffusivity will be examined and compared to experimentally measured values.

The experimental work consists of XP-9402 positive acting, chemically amplified resist that was imaged using different thermal doses.

Keywords: photoresist, Deep ultraviolet photoresist, DUV photoresist, acid catalyzed photoresist, photolithography, chemically amplified photoresist, photolithography simulation, photolithography simulator, acid diffusion

2. INTRODUCTION

Chemically amplified resists have emerged as the most likely class of resist chemistries for use in Deep-UV lithography. These resists are based on the generation of acid during exposure to light, followed by an acid catalyzed reaction during a post-exposure bake which changes the solubility of the photoresist in developer. For such systems, one molecule of photogenerated acid can cause many (possible hundreds) of subsequent reactions, thus the name "chemically amplified." An important aspect of the chemical mechanism of amplification is the diffusion of the acid.

Our lithographic work with chemically amplified resists shows key, contradictory results. In general, the profiles of these resists show very little evidence of standing waves on the side of the profile suggesting a lot of diffusion in the exposed areas, Figure 1.¹ Yet, as shown in Table 1, with increasing PEB time there is very little change in the dose to size the feature relative to when it first clears that feature, the $E_{\text{Size}}/E_{0_Effective}$ ratio,² and focus depth is stable with increasing PEB time. As acid diffusion blurs the latent image and increased deprotection shifts the portion of the latent image that is sampled to form the resist line, these two things tend to shift $E_{\text{Size}}/E_{0_Effective}$ ratio towards unity and the depth of focus towards zero. They should not stay constant. This suggests slow acid diffusion into the lower exposed regions in the resist.

Table 1: XP-9402 Lithography Results from Reference 1.

	Dose to Size 350 nm line/space pairs		Line/Space Pair Depth of Focus (μm) Nominal Feature Size			
	mJ/cm^2	$E_{\text{Size}}/E_{0_Effective}$	250	275	300	350
90°C PEB time						
30s	50.8	1.5	0.4	0.8	0.8	1.0
45s	44.4	1.5	0.4	0.8	1.0	1.2
60s	42.2	1.5	0.4	0.8	0.8	1.2
75s	39.8	1.5	0.4	0.8	1.0	1.2
90s	43.4	1.7	0.8	1.0	1.2	1.2
105s	38.9	1.6	0.4	0.8	1.0	1.2

One of the ways to reconcile this data is to envision variation in the diffusivity of the acid in the exposed and unexposed areas.

This paper will explore the impact of diffusion on the lithographic properties of generic chemically amplified resists using mathematical modeling techniques. The acid generation will be modeled as a first order reaction, and the amplification will have an arbitrary order with respect to the acid concentration. The diffusion will be modeled with constant diffusivity as well as various forms of reaction dependent diffusivities. Then a brief comparison to experimental results will be made.

3. MODEL DEVELOPMENT

3.1 RESIST KINETICS

The kinetics of the exposure and catalyzed amplification of chemically amplified photoresists have been described elsewhere^{3, 4}, but will be reviewed here for a typical case. These resists are composed of a polymer resin (possible "blocked" to inhibit dissolution), a photoacid generator (PAG), and possibly a crosslinking agent. As the name implies, the photoacid generator forms a strong acid, H^+ , when exposed to Deep-UV light. The kinetics of the reaction are thought to be standard first order:

$$\frac{\partial G}{\partial t'} = -CGI \quad (1)$$

where G is the concentration of PAG at time t' (the initial PAG concentration is G_o), I is the exposure intensity, and C is the exposure rate constant. For constant intensity, the rate equation can be solved for G :

$$G = G_o e^{-CIt'} \quad (2)$$

The acid concentration H is given by

$$H = G_o - G = G_o (1 - e^{-CIt'}) \quad (3)$$

Exposure of the resist with an aerial image $I(x)$ results in an acid latent image $H(x)$. A post-exposure bake (PEB) is then used to thermally induce a chemical reaction. This may be the activation of a crosslinking agent for a negative resist or the deprotection of the polymer resin for a positive resist. The reaction is catalyzed by the acid so that the acid is not consumed by the reaction and H remains constant. Using M as the concentration of some reactive site, these sites are consumed (i.e., are reacted) according to kinetics of some unknown order in H and first order in M :

$$\frac{\partial M}{\partial t} = -K_{amp} M H^n \quad (4)$$

where K_{amp} is the rate constant of the crosslinking reaction and t is the bake time. Simple theory would indicate that $n=1$ but the general form will be used here. Assuming H is constant, equation (4) can be solved for the concentration of reacted sites X :

$$X = M_o - M = M_o \left(1 - e^{-K_{amp} H^n t}\right) \quad (5)$$

(Note: Although H^+ is not consumed by the reaction, the value of H is not locally constant. Diffusion during the PEB causes local changes in the acid concentration, thus requiring the use of a reaction-diffusion system of equations.⁵ The approximation that H is constant is a useful one, however, which gives insight into the reaction. A more accurate reaction-diffusion approach will be presented in the following section.)

It is useful here to normalize the concentrations to some initial values. This results in a normalized acid concentration h and a normalized crosslinked concentration m :

$$h = \frac{H}{G_o} \quad x = \frac{X}{M_o} \quad m = \frac{M}{M_o} \quad (6)$$

Equations (3) and (5) become

$$\begin{aligned} h &= 1 - e^{-CI^t} \\ m &= 1 - x = e^{-\alpha h^n} \end{aligned} \quad (7)$$

where α is a lumped “amplification” constant equal to $G_o^n K_{amp} t$. The result of the PEB is an amplified latent image $m(x)$, corresponding to an exposed latent image $h(x)$, resulting from the aerial image $I(x)$.

3.2 ACID DIFFUSION

The above analysis of the kinetics of the amplification reaction assumed a locally constant concentration of acid H . Although this could be exactly true in some circumstances, it is typically only an approximation and is often a poor approximation. In reality, the acid diffuses during the bake. In one dimension, the standard diffusion equation takes the form

$$\frac{\partial H}{\partial t} = \frac{\partial}{\partial x} \left(D_H \frac{\partial H}{\partial x} \right) \quad (8)$$

where D_H is the diffusivity of acid in the photoresist. Solving this equation requires a number of things: two boundary conditions, one initial condition, and a knowledge of the diffusivity as a function of position and time.

The initial condition is the initial acid distribution within the film, $H(x, 0)$, resulting from the exposure of the PAG. The two boundary conditions are at the top and bottom surface of the photoresist film. The boundary at the wafer surface is assumed to be impermeable, giving a boundary condition of no diffusion into the wafer. The boundary condition at the top of the wafer will depend on the diffusion of acid into the atmosphere above the wafer. Although such

acid loss is a distinct possibility, it will not be treated here. Instead, the top surface of the resist will also be assumed to be impermeable.

The solution of equation (8) can now be performed if the diffusivity of the acid in the photoresist is known. Unfortunately, this solution is complicated by two very important factors: the diffusivity is a strong function of temperature and, most probably, the extent of amplification. Since the temperature is changing with time during the bake, the diffusivity will be time dependent. The concentration dependence of diffusivity could result from an increase in free volume for typical positive resists: as the amplification reaction proceeds, the polymer blocking group evaporates resulting in a decrease in film thickness but also an increase in free volume. Since the acid concentration is time and position dependent, the diffusivity in equation (8) must be determined as a part of the solution of equation (8) by an iterative method. The resulting simultaneous solution of equations (4) and (8) is called a reaction-diffusion system.

The temperature dependence of the diffusivity can be expressed in a standard Arrhenius form:

$$D_o(T) = A_r \exp(-E_a/RT) \quad (9)$$

where A_r is the Arrhenius coefficient and E_a is the activation energy. A full treatment of the amplification reaction would include a thermal model of the hotplate in order to determine the actual time-temperature history of the wafer.⁶ To simplify the problem, an ideal temperature distribution will be assumed: the temperature of the resist is zero (low enough for no diffusion or reaction) until the start of the bake, at which time it immediately rises to the final bake temperature, stays constant for the duration of the bake, then instantly falls back to zero.

The concentration dependence of the diffusivity is less obvious. Several authors have proposed and verified the use of different models for the concentration dependence of diffusion in a polymer. Of course, the simplest form would be a linear model. Letting D_o be the diffusivity of acid in completely unreacted resist and D_f the diffusivity of acid in resist which has been completely reacted,

$$D_H = D_o + x(D_f - D_o) \quad (10)$$

Another common form is the Fujita-Doolittle equation⁷ which can be predicted theoretically using free volume arguments. A form of that equation which is convenient for calculations is shown here:

$$D_H = D_o \exp\left(\frac{\alpha x}{1 + \beta x}\right) \quad (11)$$

where α and β are experimentally determined constants and are, in general, temperature dependent. Other concentration relations are also possible,⁸ but the Fujita-Doolittle expression will be used in this work.

3.3 ACID LOSS

Through a variety of mechanisms, acid formed by exposure of the resist film can be lost and thus not contribute to the catalyzed reaction to change the resist solubility. There are two basic types of acid loss: loss that occurs between exposure and post-exposure bake, and loss that occurs during the post-exposure bake.

The first type of loss leads to delay time effects -- the resulting lithography is affected by the delay time between exposure and post-exposure bake. Delay time effects can be very severe and, of course, are very detrimental to the use of such a resist in a manufacturing environment.^{9, 10} The typical mechanism for delay time acid loss is the diffusion of atmospheric base contaminants into the top surface of the resist. The result is a neutralization of the acid near the top of the resist and a corresponding reduced amplification. For a negative resist, the top portion of a line is not insolubilized and resist is lost from the top of the line. For a positive resist, the effects are more devastating. Sufficient base contamination can make the top of the resist insoluble, blocking dissolution into the bulk of the resist. In extreme cases, no patterns can be observed after development. Another possible delay time acid loss mechanism is base contamination from the substrate, as has been observed on TiN substrates.¹⁰

The effects of acid loss due to atmospheric base contaminants can be accounted for in a straightforward manner.¹¹ The base diffuses slowly from the top surface of the resist into the bulk. Assuming that the concentration of base contaminant in contact with the top of the resist remains constant, the diffusion equation can be solved for the concentration of base, B , as a function of depth into the resist film:

$$B = B_0 \exp\left(-\left(z / \sigma\right)^2\right) \quad (12)$$

where B_0 is the base concentration at the top of the resist film, z is the depth into the resist ($z=0$ at the top of the film) and σ is the diffusion length of the base in resist. The standard assumption of constant diffusivity has been made here so that diffusion length goes as the square root of the delay time.

Since the acid generated by exposure for most resist systems of interest is fairly strong, it is a good approximation to assume that all of the base contaminant will react with acid if there is sufficient acid present. Thus, the acid concentration at the beginning of the PEB, H^* , is related to the acid concentration after exposure, H , by

$$H^* = H - B \quad \text{or} \quad h^* = h - b \quad (13)$$

where the lower case symbols again represent the concentration relative to G_0 , the initial photoacid generator concentration.

Acid loss during the PEB could occur by other mechanisms. For example, as the acid diffuses through the polymer, it may encounter sights which “trap” the acid, rendering it unusable for further amplification. If these traps were in greater abundance than the acid itself, the resulting acid loss rate would be first order.

$$\frac{\partial h}{\partial t} = -K_{loss} h \quad (14)$$

where K_{loss} is the acid loss reaction rate constant. Of course, other more complicated acid loss mechanisms can be proposed, but in the absence of data supporting them, the simple first order loss mechanism will be used here.

3.4 REACTION-DIFFUSION SYSTEM

The combination of a reacting system and a diffusing system where the diffusivity is dependent on the extent of reaction is called a reaction-diffusion system. The solution of such a system is the simultaneous solution of equations (4) and (8) using equation (3) as an initial condition and equation (11) to describe the reaction-dependent diffusivity. A convenient and straightforward method to solve such equations is the finite difference method (see, for example, reference 12).

4. EXPERIMENTAL

In this work, resist images were simulated using modeling parameters derived from the conversion of dissolution rate data versus exposure dose, $R(E,z)$, to rate versus the ratio of deprotected sites to protected sites, $R(m,z)$ of the positive acting chemically amplified resist XP-9402 from Shipley Company. The method of $R(E,z)$ to $R(m,z)$ conversion is described elsewhere in this conference.¹³ Further, refinement of the parameters extracted from the $R(E,z)$ converter is accomplished by comparing the results of lithographic simulations using the range of parameter values from Table 2 against simulations using the $R(E,z)$ data for a specific thermal dose and by, also, comparing the simulated to experimental imaging results. PROLITH/2 version 4.1a was used for the lithography simulations. To do this, the thermodynamic and development parameters derived from the $R(E,z)$ to $R(m,z)$ conversion are input into the simulator. The simulations are further constrained by using a sizing dose, E_{SIZE} , from a lithography study using the same lot of resist and one of the processes that was used to get the DRM data. The E_{SIZE} from this study equaled $39.4 \text{ mJ}\cdot\text{cm}^{-2}$ for a 90°C for 90s thermal dose for $0.35\mu\text{m}$ clustered lines imaged with a $0.53\text{NA}/0.74\sigma/248.37 \text{ nm}$ GCA XLS stepper. Incidentally, this dose is in good agreement with the simulation result of $38.2 \text{ mJ}\cdot\text{cm}^{-2}$ for the same feature that was arrived at by using 90°C for 90s PEB $R(E,z)$ data set as the data base for the PROLITH/2 lithography engine¹⁴. Then using these parameters, nested multiple runs were made varying each of the

parameters within their range of finite values allowed by the R(E,z) converter. This is repeated until the simulated values converged with the results of the R(E,z) based simulation

Table 2: Modeling parameters used in PROLITH/2 version 4.1b. The initial values are from Reference 13.

Parameters	Initial Values	Final values
k_a/k_{loss}	1.2	1.2
PEB Time	90s	90s
PEB Temperature	90°C	90°C
Amplification Factor [†]	5.36	5.36
C	0.035 cm ² •mJ ⁻¹	0.035 cm ² •mJ ⁻¹
$E_{activation}$ Amplification	7.5	7.5
ln(A) Amplification	7.57	7.57
$E_{activation}$ Acid Loss	0	0
ln(A) Acid Loss	-3.0	-3.0
E_{Size}	39.4 mJ•cm ⁻²	39.4 mJ•cm ⁻²
R_{MAX}	328(±33) nm•s ⁻¹	420
R_{MIN}	-1.5(±2) nm•s ⁻¹	0.1
n	6.1(±0.5)	7
mth	0.42(±0.02)	0.42
R ²	0.93	NA

[†] Factor based on the same activation energy and pre-exponential for both processes and the change in temperature.

Experimental validation of the model was made using the following process: Coated XP-9402 to a post apply bake thickness of 792.5 nm using a MTI Multifab; this thickness corresponds to an E_{Min} on the standing wave curve. The resist's post apply bake was 115°C for 90s. Immediately after the cure, the wafers exposed using a matrix of varying focus and exposure on a 4X, 0.53NA, 0.74 coherence, 248.37 nm GCA XLS. After exposure the wafers received a 90°C for 90 s post exposure bake. Next, the wafers were developed using a 60s double process with Shipley MF-321 developer. Top-down SEM linewidth measurements of gold coated were made using an Amrrey 1880. These top-down measurements were later correlated by cross-sectional analysis on the same Amrrey 1880.

5. RESULTS AND DISCUSSION

The initial parameters from Table 2 were input into PROLITH/2 version 4.1a and refined for the constant diffusion and exponential diffusion models.

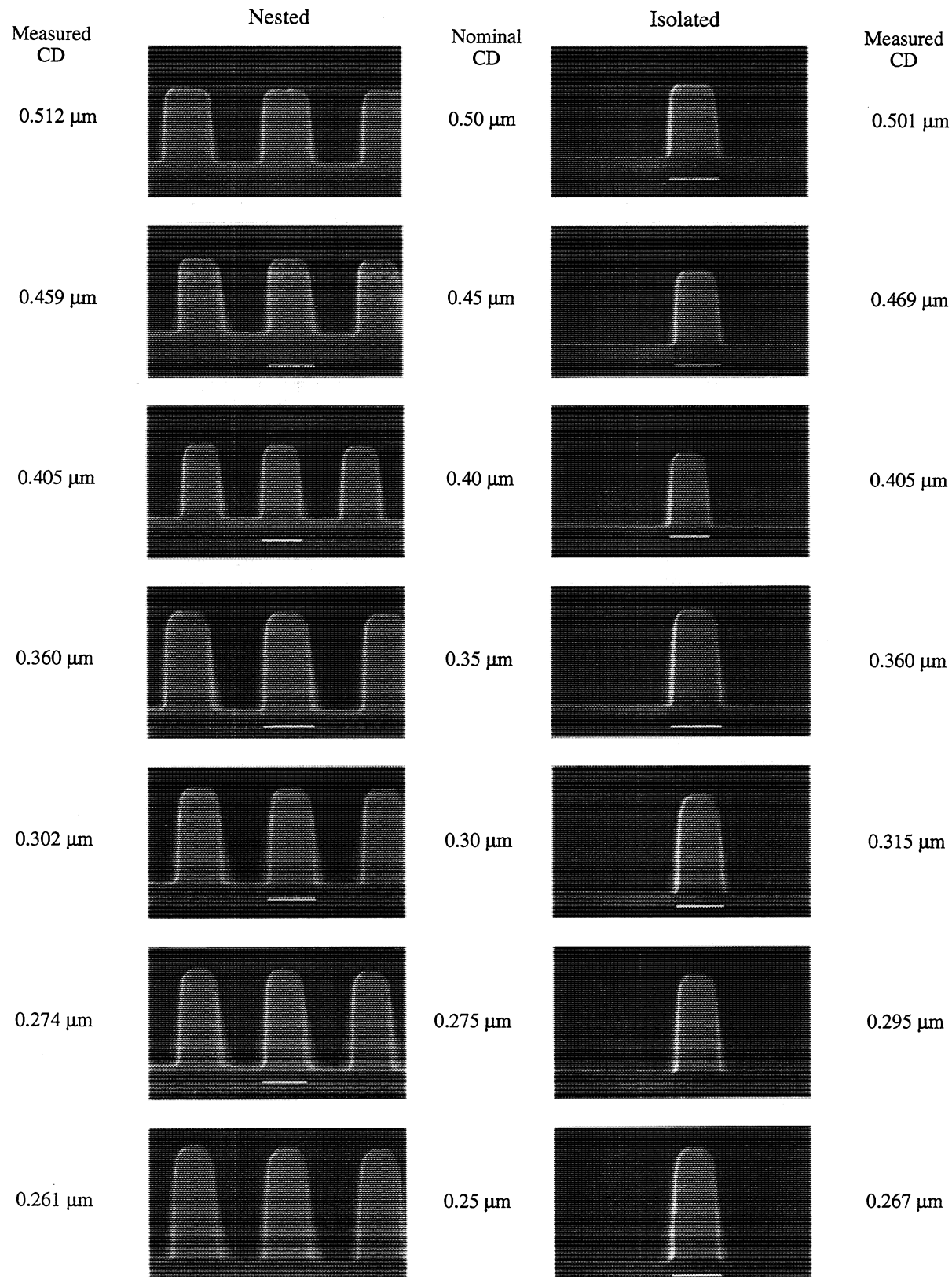


Figure 1. XP-9402 nested and isolated line linear resolution. Note: no apparent standing waves.

First, for constant diffusion, determined the diffusion coefficient needed to match E_{Size} of a 350 nm nested line for a 90s, 90°C post exposure bake. For constant diffusion the diffusion coefficient was determined to be $6.0 \text{ nm}^2 \cdot \text{s}^{-1}$ for a diffusion length of 32.8 nm. As shown in Figure 3, the simulated 250 nm nested line, $E_{\text{Size}}=42 \text{ mJ} \cdot \text{cm}^{-2}$, a diffusion length this small is not sufficient to diffuse out the standing waves. Our calculations show that at an exposure wavelength of 248 nm, to get images like those shown in Figure 1, a diffusion length of 120 nm to 130 nm is needed to minimize the standing waves on a resist image in a reaction diffusion system. Based on the constraints to the simulations provided by the parameter set and the dose to size, these diffusion lengths do not work using a constant diffusion model.

To choose which non-constant diffusion to use in the next round of simulations, the diffusivity needed to smooth the standing waves was calculated using equation (15)

$$D_0 = \frac{(\text{Diffusion_Length})^2}{2(\text{PEB_Time})} \quad (15)$$

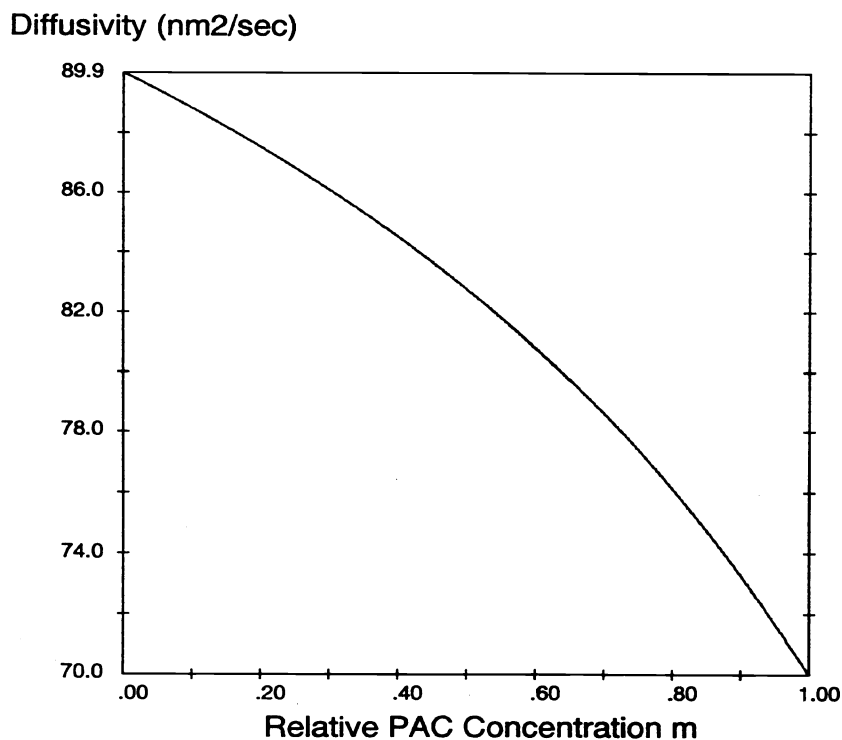
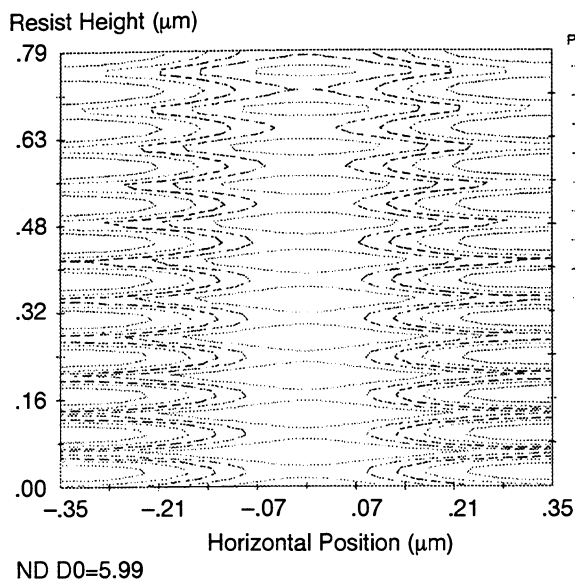


Figure 2. Typical diffusivity variation used in Figure 4.

PROLITH/2
The Positive/Negative Resist Optical Lithography Model, v4.1a



PROLITH/2
The Positive/Negative Resist Optical Lithography Model, v4.1a
Constant Diffusion

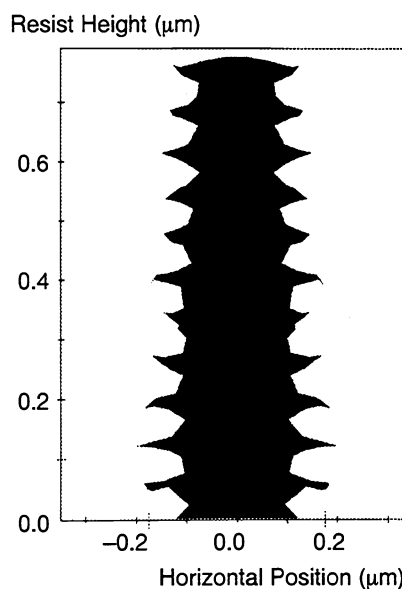
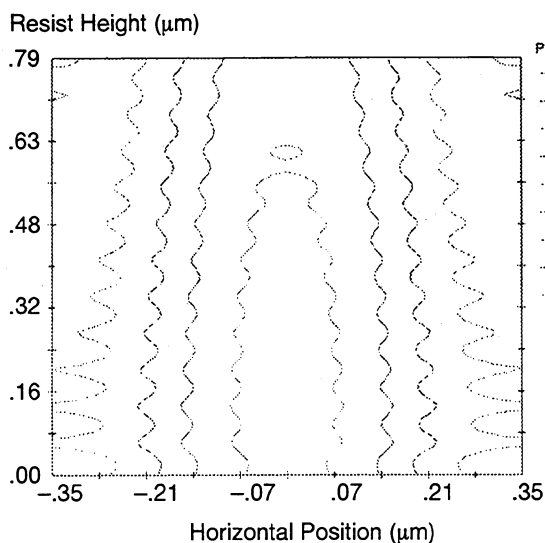


Figure 3: Simulated 250 nm nested line using constant acid diffusion. The exposure dose equals $42 \text{ mJ}\cdot\text{cm}^{-2}$ and the diffusion length equals 32.8 nm.

PROLITH/2
The Positive/Negative Resist Optical Lithography Model, v4.1a



PROLITH/2
The Positive/Negative Resist Optical Lithography Model, v4.1a
Non-Constant Diffusion

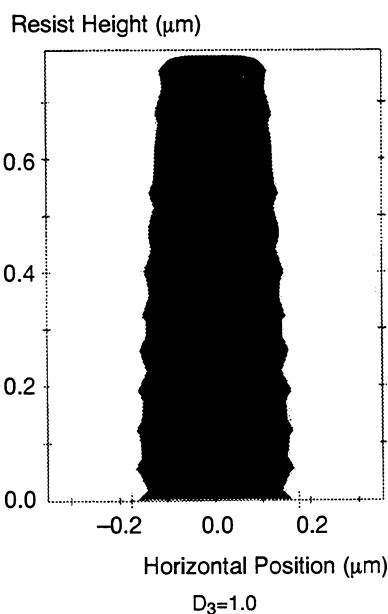


Figure 4: Simulated 250 nm nested line using exponential acid diffusion. The exposure dose equals $39.4 \text{ mJ}\cdot\text{cm}^{-2}$. The diffusion length varies from 118 nm at m of 0.76 to 127.3 nm at m of 0.

For a 120 nm diffusion length, D_0 equaled 67 to 94 $\text{nm}^2\cdot\text{s}^{-1}$. This value was set as an upper limit, corresponding to $m=0$, and the lower limit, $m=1$, was arbitrarily set to the constant diffusion value of 3.1 $\text{nm}^2\cdot\text{s}^{-1}$. Next, by examining the diffused latent image in Figure 3, we determined the post exposure baked latent image's 0.76 m value contour to be the one that ultimately forms the outer surface of the developed resist image with this parameter set. Next, using PROLITH/2 4.1b we varied the slope of the exponential diffusion model such that at the 0.76 m value that the diffusivity was at least 60 $\text{nm}^2\cdot\text{s}^{-1}$ and at 0.6 m, that the value was in the neighborhood of 80 to 90 $\text{nm}^2\cdot\text{s}^{-1}$. Figure 4, using an E_{Size} of 39.4 $\text{mJ}\cdot\text{cm}^2$, shows a 250 nm nested line with smoother standing waves. Note that the top of this simulated image is rounded and that the entire profile is similar to the 250 nm images in Figure 1. The diffused latent image simulation indicates that the image is rounded because of the resists high non-functional absorbance and because the more highly exposed resist at the top of the resist also has more acid diffusion than at the bottom of the resist. This result suggests that the exponential model may be a good predictor of lithographic performance for the XP-9402.

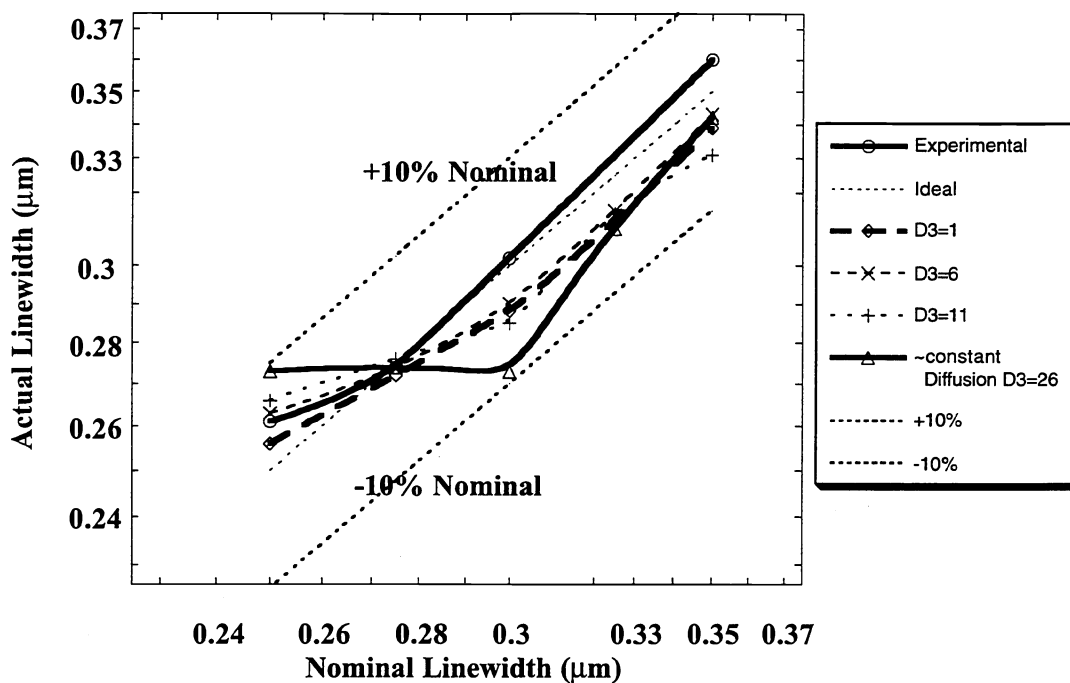


Figure 5: Comparison of simulated and experimental linear resolution. Note a log-log plot has been used to show the data.

But one image does not a definitive result make. To test out the model further, we simulated a linear resolution data set at best focus and compared it to experimental values, see Figure 5. These data show that the constant diffusion case can not resolve the 250 nm nested lines at the dose that sizes the 350 nm feature. However, all the different exponential slopes, D_3 , examined showed similar behavior to the experimental results. Of these curves D_3 equal to 6 appears to be the most reasonable.

As a final validation, a focus exposure matrix was simulated and compared to experimental results for 250 nm nested lines. These data are shown in Figure 6. Within $\pm 0.5 \mu\text{m}$ of focus and from $\pm 10\%$ of exposure these two data sets compare quite closely. $1 \cdot E_0$ Effective, where the feature first opens, is the same. E_{Size} is within $1 \text{ mJ} \cdot \text{cm}^2$ of the experimental value and the isofocal regions are within 10 nm of each other. The simulation is more optimistic in its prediction than what is observed experimentally. There are many reasons for this over prediction: One is that lens flair, coma and astigmatism not accounted for. Another reason is the optical simulator used for this simulation was a scalar model, without adjustments for high lens NA situation, so that the simulated images are more tolerant to bulk focus effects compared to the experimental results. In general, these results however, are the best that we have been able to achieve to date with any simulator.

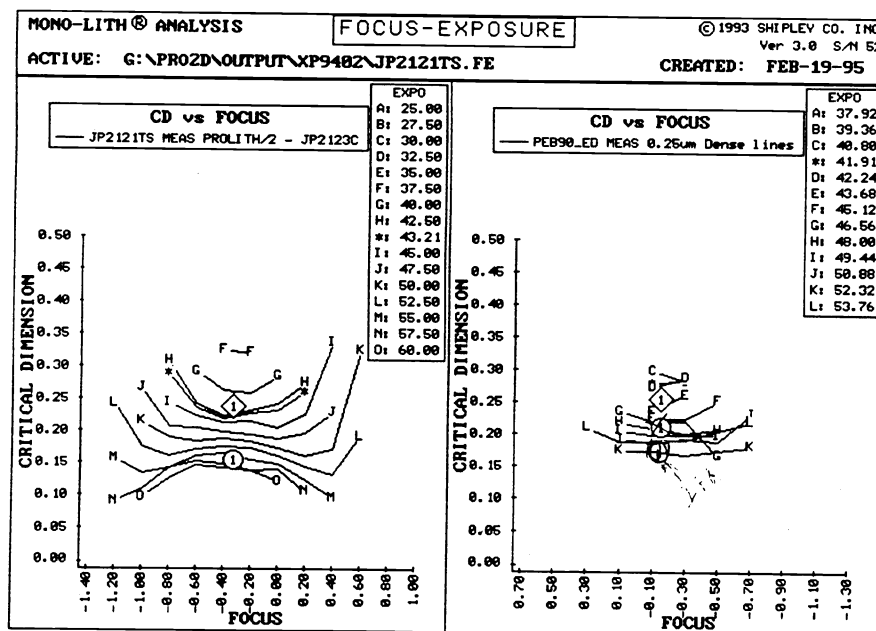


Figure 6. Focus-Exposure Matrix data comparing simulation to experiment.

Conclusions

Based on the parameters that were derived using the R(E,z) converter and data rate file input for lithographic simulation to attain dose to size, diffusivity solutions were found using the three different diffusion models.

Comparing linearity results suggest that based on the our parameter set the best model for simulating this particular lithographic process was the exponential model for acid diffusivity.

Depth of focus comparisons also suggest that the exponential model is better than the constant diffusion model, but that there are more effects to be considered to get the best emulation to the real imaging process.

References

- ¹ J. S. Petersen, T. H. Fedynyshyn, J. W. Thackeray, P. Freeman, D. A. Miller, "Design Issues for Making a Robust 248nm Acid Catalyzed Positive Photoresist", MicroProcess Conference'94, Hsinchu, Republic of China, 1994.
- ² J. S. Petersen: Optical/Laser Microlithography II, Burn J. Lin, Editor, Proc. SPIE 1088, pp.540-567 (1989).
- ³ R. A. Ferguson, J. M. Hutchinson, C. A. Spense, and A. R. Neureuther, *J. Vac. Sci. Technol. B* 8, 1423 (1990).
- ⁴ D. Ziger, C. A. Mack, and R. Distasio, Proc. SPIE 1466, 270 (1991).
- ⁵ E. Barouch, U. Hollerbach, S. A. Orszag, M. T. Allen, and G. S. Calabrese, Proc. SPIE 1463, 336 (1991).
- ⁶ C. A. Mack, D. P. DeWitt, B. K. Tsai, and G. Yetter, "Modeling of Solvent Evaporation Effects for Hot Plate Baking of Photoresist," *Advances in Resist Technology and Processing XI, Proc.*, SPIE Vol. 2195 (1994) pp. 584-595.
- ⁷ H. Fujita, A. Kishimoto, and K. Matsumoto, "Concentration and Temperature Dependence of Diffusion Coefficients for Systems Polymethyl Acrylate and n-Alkyl Acetates," *Transactions of the Faraday Society*, Vol. 56 (1960) pp. 424-437.
- ⁸ D. E. Bornside, C. W. Macosko and L. E. Scriven, "Spin Coating of a PMMA/Chlorobenzene Solution," *Journal of the Electrochemical Society*, Vol. 138, No. 1 (Jan., 1991) pp. 317-320.
- ⁹ S. A. MacDonald, et al., "Airborne Chemical Contamination of a Chemically Amplified Resist," *Advances in Resist Technology and Processing VIII, Proc.*, SPIE Vol. 1466 (1991) pp. 2-12.
- ¹⁰ K. R. Dean and R. A. Carpio, "Contamination of Positive Deep-UV Photoresists," *OCG Microlithography Seminar Interface '94, Proc.*, (1994) pp. 199-212.
- ¹¹ T. Ohfuji, A. G. Timko, O. Nalamasu, and D. R. Stone, "Dissolution Rate Modeling of a Chemically Amplified Positive Resist," *Advances in Resist Technology and Processing X, Proc.*, SPIE Vol. 1925 (1993) pp. 213-226.
- ¹² F. P. Incropera and D. P. DeWitt, Fundamentals of Heat and Mass Transfer, 3rd edition, John Wiley & Sons (New York: 1990).
- ¹³ John S. Petersen, Chris A. Mack, James W. Thackeray, Roger Sint, Theodore H. Fedynyshyn, J. Michael Mori, Jeffrey D. Byers and Daniel A. Miller: "Characterization and modeling of a positive acting chemically amplified resist", 2438-45, SPIE
- ¹⁴ FINLE Technologies, Inc., Austin, Texas, 78716